International Journal of Nanomedicine

Dovepress
open access to scientific and medical research

Open Access Full Text Article

ORIGINAL RESEARCH

Enhanced antifungal effects of amphotericin B-TPGS-b-(PCL-ran-PGA) nanoparticles in vitro and in vivo

This article was published in the following Dove Press journal:
International Journal of Nanomedicine
24 November 2014
Number of times this article has been viewed

Xiaolong Tang[1,2,*]
He Zhu[3,*]
Ledong Sun[4,*]
Wei Hou[2]
Shuyu Cai[1]
Rongbo Zhang[1]
Feng Liu[5]

[1]Stem Cell Engineering Research Center, School of Medicine, Anhui University of Science and Technology, Huainan, People's Republic of China; [2]State Key Laboratory of Virology, Life Sciences College, Wuhan University, Wuhan, Hubei, People's Republic of China; [3]Institute of Skin Damage and Repair, General Hospital of Beijing Military Command, Beijing, People's Republic of China; [4]Department of Dermatology, Zhujiang Hospital, Southern Medical University, Guangzhou, Guangdong, People's Republic of China; [5]Department of Anesthesiology, Children's Hospital, Chongqing Medical University; Key Laboratory of Child Development and Disorders of the Ministry of Education, Chongqing, People's Republic of China

*These authors contributed equally to this work

Background: Amphotericin B (AMB) is a polyene antibiotic with broad spectrum antifungal activity, but its clinical toxicities and poor solubility limit the wide application of AMB in clinical practice. Recently, new drug-loaded nanoparticles (NPs) – diblock copolymer D-α-tocopheryl polyethylene glycol 1000 succinate-b-poly(ε-caprolactone-ran-glycolide) (PLGA-TPGS) – have received special attention for their reduced toxicity, and increased effectiveness of drug has also been reported. This study aimed to develop AMB-loaded PLGA-TPGS nanoparticles (AMB-NPs) and evaluate their antifungal effects in vitro and in vivo.

Methods: AMB-NPs were prepared with a modified nanoprecipitation method and then characterized in terms of physical characteristics, in vitro drug release, stability, drug-encapsulation efficiency, and toxicity. Finally, the antifungal activity of AMB-NPs was investigated in vitro and in vivo.

Results: AMB-NPs were stable and spherical, with an average size of around 110 nm; the entrapment efficacy was closed to 85%, and their release exhibited a typically biphasic pattern. The actual minimum inhibitory concentration of AMB-NPs against *Candida albicans* was significantly lower than that of free AMB, and AMB-NPs were less toxic on blood cells. In vivo experiments indicated that AMB-NPs achieved significantly better and prolonged antifungal effects when compared with free AMB.

Conclusion: The AMB-PLGA-TPGS NP system significantly improves the AMB bioavailability by improving its antifungal activities and reducing its toxicity, and thus, these NPs may become a good drug carrier for antifungal treatment.

Keywords: drug delivery, anti-infection, nanocarrier, *C. albicans*, amphotericin B

Introduction

Candida spp. are major human opportunistic pathogens that cause both mucosal and deep tissue infections. The incidence of mucosal and cutaneous fungal infections increasing dramatically worldwide, especially in patients who are immunocompromised because of cancer chemotherapy, immunosuppressive therapy after organ transplantation, or human immunodeficiency virus infection.[1,2] Most of these infections are caused by *Candida albicans*, non-*albicans Candida* spp., *Candida tropicalis, Candida glabrata,* and *Candida Krusei*.[3,4] Echinocandins, polyenes, pyrimidine, allylamine, and azoles are the most common antifungal agents available for the treatment of topical *Candida* spp. infections. However, these antifungal drugs have several defects in clinical practice, such as low efficacy and serious adverse drug reactions (ADRs) and even the emergence of resistant strains. This upward trend is concerning considering the limited number of antifungal drugs available.[5] Therefore, there is an urgent need for the development of new antifungal agents.

Correspondence: Feng Liu
Department of Anesthesiology of Children's Hospital of Chongqing Medical University, No 136 Zhongshan No 2 Road, Chongqing 400014, People's Republic of China
Email liu781234@sina.com

Among all antifungal agents, amphotericin B (AMB) still remains the most important drug. AMB, at 15–20 mg/kg, has to be given by intravenous infusions either daily or on alternate days, necessitating prolonged hospitalization. In addition, ADRs, such as kidney damage, hypokalemia, and even thrombophlebitis, are also common and may be occasionally serious.[5] The lipid formulations of AMB may alleviate the toxicity and increase the bioavailability of AMB.[5,6] Nevertheless, the high cost of these formulations puts them beyond the reach of most of patients with fungal infection.

With the development of copolymer nanoparticles (NPs), nanosuspension formulations of AMB, such as with poly(D,L-lactide-co-glycolide) (PLGA), polylactide (PLA) and polyglycolide (PGA), carbon nanotubes, poly(ethylene glycol)-block-poly(caprolactone), and poly (ethylene glycol)-block-poly(D,L-lactic acid), have been found to be able to improve the solubility of AMB. However, this reduces the tissue fungal burden by no more than 30% as compared with controls, indicating limited in vivo efficacy of these formulations.[5–7] In addition, the stability, tissue permeability, degradation rate, and toxicity of NPs themselves are also concerns in this field.[8–10] The recently developed diblock copolymer D-α-tocopheryl polyethylene glycol 1000 succinate-b-poly(ε-caprolactone-ran- glycolide) (TPGS-b-(PCL-ran-PGA) [hereafter, referred to as PLGA-TPGS]) has received special attention as a promising antimicrobial agent, due to its good biocompatibility and biodegradability.[7] Therefore, the synthesis of uniform PLGA-TPGS copolymer NPs (PLGA-TPGS NPs) with specific requirements in terms of size, shape, and physical and chemical properties is of great interest in the development of new drugs.[8,9] A variety of studies[8–10] have shown they have good biocompatibility and biodegradability and excellent targeted drug delivery, but the antifungal effects of AMB-loaded PLGA-TPGS NPs (AMB-NPs) are mostly unknown. In this study, AMB-NPs were synthesized, and their antifungal effects on the *Candida* spp. of clinical isolates and on American Type Culture Collection (ATCC) strains were investigated.

Materials and methods

Materials

AMB and coumarin-6 were purchased from Sigma-Aldrich Co. (St Louis, MO, USA). PLGA-TPGS (molecular weight: ~23,000 Da) copolymer was obtained from the Graduate School at Shenzhen, Tsinghua University, Beijing, People's Republic of China. Acetonitrile and methanol (Chromatogram analytical pure [AR], high-performance liquid chromatography [HPLC] grade) were purchased from EM Science (Gibbstown, NJ, USA). All other agents were of analytical grade or higher quality and commercially available. Millipore water was prepared by a Milli-Q Plus System (Millipore Inc., Billerica, MA, USA). *C. albicans* was obtained from the ATCC (ATCC 10231; Rockville, MD, USA).

Preparation of AMB-NPs

D-α-tocopheryl polyethylene glycol 1000 succinate (TPGS) is a water-soluble derivative of the natural form of D-α-tocopherol and can improve the aqueous solubility of hydrophobic drugs, such as AMB and steroids,[8,9] and hydrophobic AMB can be effectively connected to hydrophobic PLA. Thus, PLA-TPGS, having both hydrophilic and hydrophobic groups, can self-aggregate due to its intramolecular and/or intermolecular hydrophobic interactions with hydrophobic drugs, such as AMB. A modified nanoprecipitation method was used to entrap AMB into the PLGA-TPGS NPs.[10,11] Briefly, a preweighed amount of AMB powder and 100 mg of PLGA-TPGS copolymer were dissolved in 10 mL of acetone by adding into the dispersing phase (10 mL of anhydrous ethanol), under moderate sonication and stirring at room temperature. This mixture was added into 60 mL of 0.05% nonsolvent-TPGS aqueous solution, under stirring. The resulting NP suspension was stirred at room temperature overnight to remove acetone completely. The NP suspension was centrifuged at 23,000 rpm for 20 minutes and then washed thrice to remove the emulsifier and unloaded drug. At the end, the dispersion was lyophilized for 48 hours for further use.

Characterization of AMB NPs

NP characterization and drug content and entrapment efficiency

All measurements were taken at room temperature after equilibration for 10 minutes. Average size and zeta potential (ZP) of different NPs were analyzed using a dynamic light-scattering detector (Zetasizer ZS90; Malvern Instruments Ltd, Malvern, UK). Data were obtained from three averaged measurements. The surface morphology of NPs was examined by a field emission scanning electron microscopy (FESEM) (JSM-6301F; JEOL, Tokyo, Japan). To prepare samples for FESEM, the NPs were fixed on the stub by a double-sided sticky tape and then coated with a platinum membrane, using a JFC-1300 automatic fine platinum coater (JEOL). Morphological examination of the PLA-TPGS NPs was performed by transmission electron microscopy (H600; Hitachi Ltd, Tokyo, Japan).

To determine the drug-loading content (LC) and the entrapment efficiency (EE%) of AMB-NPs, a predetermined

amount of NPs were dissolved in 1 mL of methylene dichloride, under vigorous vortexing. This solution was transferred into 5 mL of acetonitrile and deionized water (50:50 [v/v]). A nitrogen stream was introduced, to evaporate the methylene dichloride, for approximately 20 minutes. Then, a clear solution was obtained for HPLC (LC 1200; Agilent Technologies, Santa Clara, CA, USA). A reverse-phase C_{18} column (250×4.6 mm, 5 µm, C_{18}; Agilent Technologies) was used, at 25°C. The flow rate of the mobile phase was 1 mL/min. The column effluent was detected by using an ultraviolet detector, at the λ_{max} of 297 nm. The measurement was performed in triplicate. LC and EE% of the drug-loaded NPs were calculated according to the following equation:

$$EE\% = \frac{(\text{weight of AMB in the NPs})}{(\text{weight of the feeding AMB})} \times 100\%. \quad (1)$$

Drug-release assay

The in vitro release of AMB from the AMB-NPs was determined by measuring the amount of residual AMB in the NPs.[12] In brief, 5 mg of lyophilized AMB-loaded NPs were transferred into a centrifuge tube and redispersed in 8 mL of phosphate buffer solution (PBS) (pH 7.4) containing 0.1% (w/v) Tween® 80. The tube was vibrated at 135 rpm, at 37°C. At certain time intervals, the tube was centrifuged at 25,000 rpm for 15 minutes. The supernatant was then transferred into a glass test tube for HPLC. The pellet was resuspended in 8 mL of fresh PBS for subsequent analysis. The accumulative release of AMB from NPs was plotted against time.

Toxicity study in vitro

In vitro toxicity of free AMB and AMB-NPs was determined with a previously reported method.[12] Briefly, blood samples were collected from mice and anticoagulated with heparin. Then, 0.4 mL of PBS containing free AMB or AMB-loaded nanospheres at different concentrations (0–0.4 mg/mL) were mixed with 0.6 mL of 0.2% red blood cells (v/v) suspension, followed by incubation for 72 hours. The hemolytic effects were determined by measurement of optical density at 450 nm, with a spectrophotometer (model 1700; Shimadzu Corp, Kyoto, Japan). The hemolysis rate (%) was calculated as follows:

$$\text{Hemolysis rate (\%)} = \frac{\begin{array}{l}(\text{mean of compound NP group} - \\ \text{mean of negative control group})\end{array}}{\begin{array}{l}(\text{mean of positive control group} - \\ \text{mean of negative control group})\end{array}} \times 100\%. \quad (2)$$

Detection of apoptosis markers in *C. albicans*

C. albicans spores (1×10^6 spores/mL) were inoculated in Roswell Park Memorial Institute (RPMI) 1640 medium, at 37°C for 5 hours, with and without AMB-NPs (10.0 µg/mL) and incubated for 12 hours at 37°C, with vibration at 180 rpm. After incubation for 12 hours, *C. albicans* were harvested and washed twice with PBS (pH 7.4). Then, *C. albicans* were digested by incubation with a lysis buffer (1.2 U of chitosanase, 1.3 U of chitinase, 1.5 U of lyticase, and 10 mg/mL lysing enzyme) (Sigma-Aldrich Corp) for 5 hours at 30°C and analyzed for the apoptosis, after annexin V/propidium iodide (PI) staining. In brief, 20 µL of annexin V-FITC (50 µg/mL) (Annexin V FITC Apoptosis Detection Kit; BD Pharmingen™, San Diego, CA, USA) and 20 µL of PI (200 µg/mL) were mixed with 1 mL of cell suspension, followed by incubation for 20 minutes in the dark, at room temperature.[13–15] The apoptotic cells showed green fluorescence and necrotic cells showed red fluorescence, as described by Khan et al and Shirazi and Kontoyiannis.[13,14] The samples were detected by fluorescence microscopy or flow cytometry (BD Biosciences).

Antifungal activity in vitro

Antifungal activity in vitro was tested by paper-plate technique. Briefly, 10 µL of *C. albicans* conidial suspension (1×10^5 spores/mL) was spread over the glucose agar. Then, 5 mm diameter filter paper was made with a sterile borer and sterilized. Three papers were placed on the agar. The minimum inhibitory concentration (MIC) of AMB for *C. albicans* is 0.2–1.0 µg/mL,[16] and thus 2.5, 5, 10, 20, and 40 µL of AMB-NPs, at 10.6 µg/mL (equivalent to 1.0 µg/mL AMB), and free AMB, at 1.0 µg/mL, were separately dropped onto the filter paper, followed by incubation for 4 hours at room temperature. Then, the plates were incubated at 28°C for 9 days, and digital photographs were taken. The antifungal activity was evaluated every day. The antifungal activity of AMB-NPs was compared with that of free AMB.

Toxicity study in vivo and animal studies

In vivo therapeutic efficacy of AMB-NPs was tested with a described method.[17] In brief, BALB/c mice (weight: 20–22 g; age: 6–8 weeks) were purchased from the Experimental Animal Center of Anhui Medical University (Hefei, Anhui, People's Republic of China). They were given access ad libitum to food and water. The Animal Ethics Committee of Anhui University approved all the animal studies, and

procedures conformed to the Guide for the Care and Use of Laboratory Animals published by the US National Institute of Health. Starting at 3 days before treatment, 50 BALB/c mice were infected by inhalation of 20 µL of PBS containing 1.0×10^6 fungi, for 3 days. These mice were then randomly divided into six groups: mice in group 1 were treated with PBS (1.0 mg/kg, pH=7.4); mice in group 2 were treated with free AMB (1 mg/kg/day for 10 days, totaling 10.0 mg/kg/animal); mice in group 3 were treated with null-loaded NPs (10.0 mg/kg on the first, seventh, and 14th days, and totaling 30 mg/kg/animal); mice in group 4 were treated with AMB-NPs (10.0 mg/kg on the first, seventh, and 14th days, and totaling 30 mg/kg/animal, equivalent to AMB 3.0 mg/kg/animal); mice in group 5 were not treated after infection; and group 6 was the control group. All these treatments were intravenously carried out at 24 hours after the last fungal challenge. At the end of the experiment, the surviving mice were anesthetized and sacrificed. Then, the fungal colony forming units (CFU) in the liver, kidney, heart, and right lung were determined, and the left lung was collected, embedded in paraffin and sectioned at 3 µm, followed by hematoxylin and eosin (HE) staining.

To determine the median lethal dose (LD_{50}), mice were intravenously treated with 0.5 mL of AMB-NPs in saline at different concentrations (10, 20, 40, 80, 160, 320, and 640 mg/kg, n=10 per group). The survival time of each animal was recorded up to 14 days after treatment, and the total number of dead animals was recorded, to calculate the lethal dose for 50% of animals (LD_{50}).

In all toxicity assays, the control mortality rate was corrected for, using the following formula:

$$\text{Corrected mortality} = \frac{(\text{alive in control mice \%} - \text{alive in treated mice \%})}{\text{alive in control mice \%}}. \quad (3)$$

Statistical analysis

Qualitative data were expressed as means ± standard deviation. Differences between two groups were analyzed by Student's *t*-test. A value of $P<0.05$ was considered statistically significant. Statistical analysis was performed with SPSS for Windows, Version 11.0.

Results

NP characteristics: morphology, size, ZP, EE, and release

The size and surface properties of NPs play a crucial role in drug-release kinetics, cellular uptake behavior, in vivo pharmacokinetics, and tissue distribution.[18] The physical properties of the AMB-NPs are displayed in Figure 1 and Table 1. The average hydrodynamic size of AMB-NPs was ~120–130 nm in diameter, which is in an excellent size range for ready accumulation in the tumor vasculature, due to enhanced permeation and retention effects.[19] ZP is an important predictor of the dispersion stability of NPs. A high ZP means high surface charge. The ZP distribution of AMB-NPs is shown in Table 1 and ranged from −18 mV to −19 mV. As shown in Table 1, the LC and the EE% of the AMB-NPs

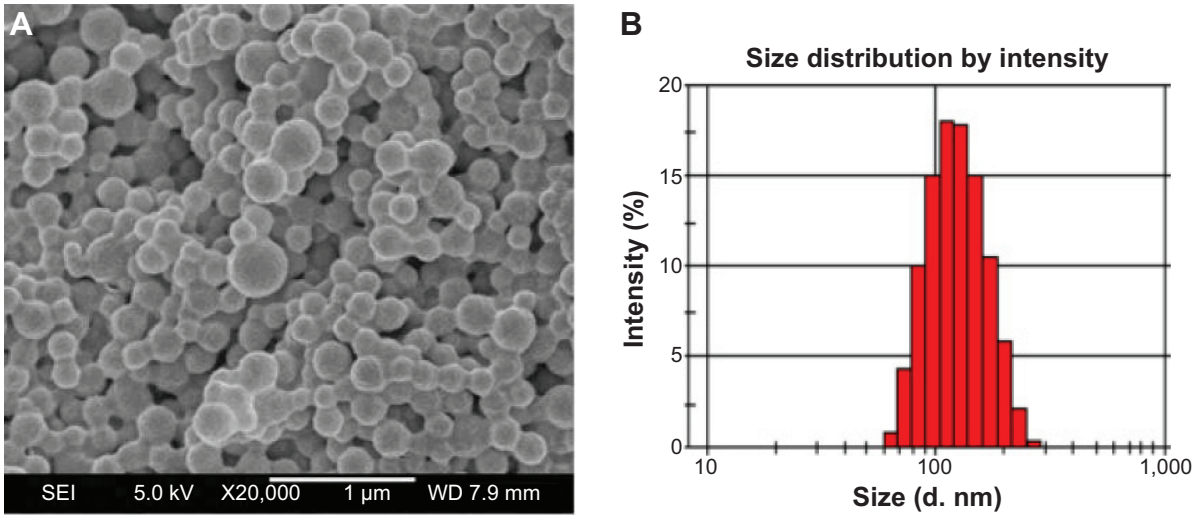

Figure 1 Physical properties of AMB-NPs.
Notes: (**A**) Representative FESEM image of AMB-NPs. (**B**) Hydrodynamic particle size of AMB-coated nanoparticles as measured by dynamic light scattering.
Abbreviations: AMB, amphotericin B; FESEM, field emission scanning electron microscopy; NPs, nanoparticles; SEI, secondary electron image; d.nm, diameter (nm).

Table 1 Characteristics of AMB-loaded nanoparticles (n=3)

Polymer	Particle size (nm) mean ± SD	PDI	ZP (mV) mean ± SD	LC (%)	EE (%)
PLGA-TPGS	115.2±4.7	0.247	−22.9±0.7	–	–
AMB-PLGA-TPGS	122.7±3.9	0.199	−18.5±0.6	9.45	84.37

Abbreviations: AMB, amphotericin B; EE, entrapment efficiency; LC, loading content; PDI, polydispersity index; PLGA, poly(d, l-lactide-co-glycolide); SD, standard deviation; TPGS, d-α-tocopheryl polyethylene glycol 1000 succinate; ZP, zeta potential.

were higher than those of previously reported NPs,[11–15] indicating a higher affinity between the star-shaped core region of PLGA and hydrophobic AMB. Moreover, the LC reached approximately 10.0%, and EE% reached approximately 85%, suggesting an ideal delivery vehicle for drugs. The particle size and size distribution of AMB-NPs were detected by dynamic light scattering, and the data are displayed in Table 1. According to the polydispersity index, ZP (mV), particle size (nm), LC (%), and EE% PLGA-TPGS copolymer NPs had advantages as an efficient vehicle for drug delivery. To detect the stability of the drug-loaded NPs, AMB-NPs were dispensed in PBS. Our results showed the mean size and size distribution of AMB-NPs remained unchanged within 5 months. Moreover, the average size and size distribution of AMB-NPs at 4°C remained unchanged on days 30, 60 and 90. These findings suggest that AMB-NPs have good stability and redispersion ability.

In vitro drug release

The in vitro drug release of the freshly prepared AMB-NPs in PBS containing 0.1% w/v Tween 80 (pH 7.4) was detected within the first 22 days, and the results are displayed in Figure 2. Tween 80 was applied to improve the solubility of AMB in PBS and to avoid the adhesion of AMB onto the tube wall.[20] The AMB release from AMB-NPs displayed an initial burst of 58.3% in the first 12 days, followed by a slow-release phase sustained for up to 30 days, which was predominantly attributed to the diffusion of AMB. After 30 days, the accumulative AMB release from NPs reached 66.4%, which indicated that the polymer PLGA-TPGS-NPs has favorable drug-release capability.

Drug toxicity in vitro and in vivo

The hemolytic ability of free AMB and AMB-NPs is shown in Figure 3. The maximum hemolytic ability (100% lysis) of AMB and AMB-NPs was 60 μg/mL and 500 μg/mL, respectively, but null-loaded NPs had no hemolytic ability (1.0% lysis of erythrocytes) up to 1.0 mg/mL. As shown in Figure 3, AMB-NPs showed no toxicity (<2.0% lysis of erythrocytes) when their concentration was less than 120 μg/mL, and the proportion of lysed erythrocytes was only 50% when the AMB-NP concentration was as high as 350 μg/mL.

In order to assess the potential toxicity, BALB/c mice were intravenously injected with AMB-NPs at different doses, and the survival rate was determined. A significant difference in the survival rate was observed between the AMB-NP group and free AMB treatment group within 2 weeks after treatment ($P<0.05$). The mortality was 10.0%, 25.0%, and 50.0% in mice treated with AMB-NPs at 80 mg/kg, 150 mg/kg, and 200 mg/kg, respectively, but the morality was 20% and 50% in mice treated with free AMB at 10 mg/kg and 20 mg/kg, respectively, while there was no death in mice treated with null-loaded NPs (0–1.0 g/mL). The LD_{50} was 20.0 mg/kg for free AMB and 260.0 mg/kg for AMB-loaded NPs. Therefore, when compared with free AMB, the AMB-NPs are safer in clinical antifungal therapy.

In vitro antifungal activity

To evaluate the antifungal activity of AMB-NPs, the MIC of free AMB, AMB-NPs, and empty PLGA-TPGS copolymer NPs was tested in *C. albicans*. As shown in Table 2, the MIC of AMB-NPs was similar to that of free AMB, indicating that AMB-NPs have an antifungal activity similar to free

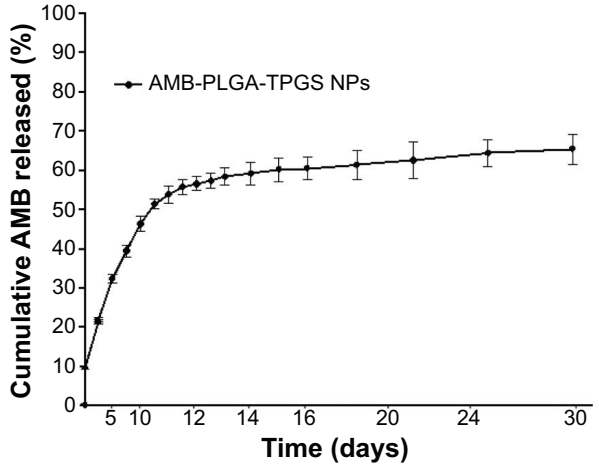

Figure 2 Cumulative release of AMB-PLGA-TPGS nanoparticles (AMB-NPs) (mean ± SD, n=5).

Abbreviations: AMB, amphotericin B; NP, nanoparticle; PLGA, poly(d, l-lactide-co-glycolide); SD, standard deviation; TPGS, d-α-tocopheryl polyethylene glycol 1000 succinate.

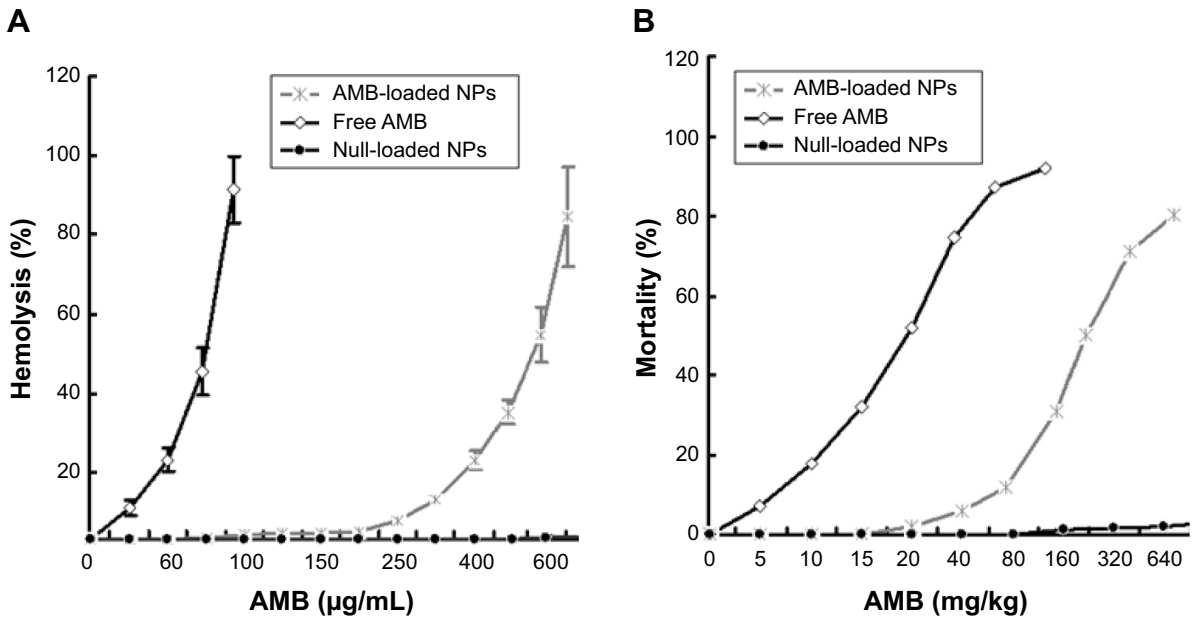

Figure 3 Percentage of hemolysis and mortality related to null-loaded NPs, AMB in free and AMB-loaded NP forms.
Notes: (**A**) Hemolysis related to null-loaded NP, free AMB and AMB-loaded NP forms. Data were from three independent experiments. (**B**) Determination of LD_{50}. The LD_{50} of null-loaded NPs, free AMB and AMB-loaded NPs was >1,000 mg/kg, 20 mg/kg, and 200 mg/kg, respectively, in healthy mice (n=10).
Abbreviations: AMB, amphotericin B; LD_{50}, lethal dose for 50% of animals; NP, nanoparticle.

AMB and that the PLGA-TPGS copolymer did not affect the antifungal activity of polymeric NPs. Of note, in the first 10 days, AMB released from AMB-NPs was less than 50%. Thus, above findings suggest the MIC of AMB-NPs is much lower than that of free AMB.

To investigate whether the drug can effectively induce apoptosis and necrosis of *C. albicans* cells, the apoptosis and necrosis of AMB-NPs-treated *C. albicans* were detected after annexin V-FITC and PI double-staining. Apoptotic cells were positive for annexin V-FITC, whereas necrotic cells were positive for PI.[21] Following AMB-NPs (5.0 μg/mL, equivalent to 0.5 μg/mL free AMB) exposure at 37°C for 24 hours, about 76% of *C. albicans* were positive for annexin V-FITC, while only 40% of *C. albicans* were positive for PI. However, after AMB-NP treatment for 48 hours, almost of all the *C. albicans* were positive for annexin V-FITC, and about 85% for PI, as showed in Figure 4A. After AMB-NP treatment for 72 hours, almost all of the *C. albicans* were positive for annexin V-FITC, but the fluorescence intensity reduced significantly, and nearly all of the cells were positive for PI, as shown in Figure 4A; flow cytometry showed similar results (Figure 4B). These results suggest that AMB-NPs induce apoptosis and necrosis in a time-dependent manner in *C. albicans* cells.

Table 2 MIC free AMB and AMB-loaded nanoparticles against *Candida albicans*

Component	MIC (μg/mL, n=3)
Free AMB	0.48
AMB-NPs	5.0 (equivalent to 0.5 μg/mL free AMB)
Empty PLGA-TPGS nanoparticles	>10.0

Abbreviations: AMB, amphotericin B; MIC, minimum inhibitory concentration; NP, nanoparticle; PLGA, poly(d, l-lactide-co-glycolide); TPGS, d-α-tocopheryl polyethylene glycol 1000 succinate.

Therapeutic efficacy of AMB-NPs in *C. albicans* infection

The therapeutic efficacy of AMB-loaded NPs was evaluated by comparison of *C. albicans*–infected mice with and without therapy. Results showed a significant reduction in the CFU of different organs, especially the kidney and spleen (Table 3), after AMB-NP therapy. The mortality of *C. albicans*-infected mice without AMB therapy was 100% after 10 days, whereas survival rate of *C. albicans*-infected mice treated with free AMB and AMB-NPs was 30.0 and 80.0%, respectively. The differences in the antifungal potency and toxicity between free AMB and AMB-NPs may be ascribed to the high stability of AMB-NPs.[20,21]

Interestingly, the fungal burden of different organs also favored that both free AMB and AMB-NPs could reduce the amount of bacteria in the lung, kidney, heart, and liver. However, the fungal burden of free AMB-treated mice was significantly higher than that of AMB-NP-treated mice

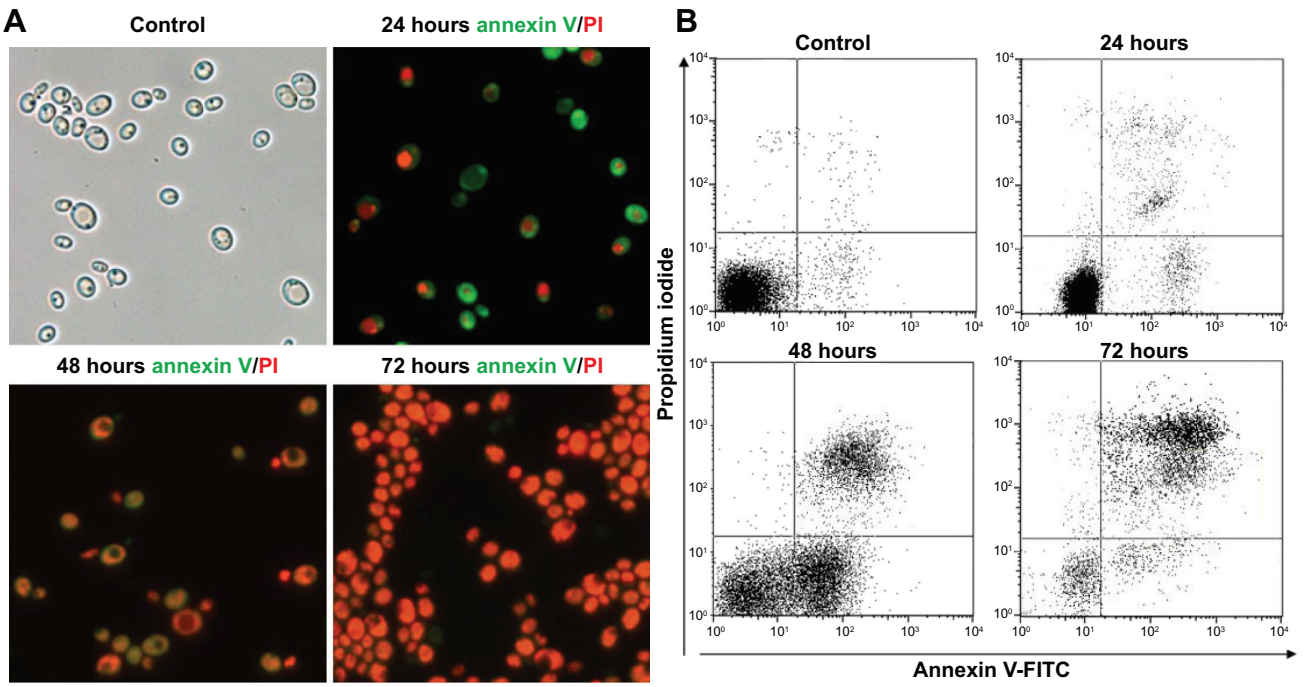

Figure 4 Representative photographs of AMB-treated *Candida albicans*.
Notes: (**A**) Bright-field photographs of *C. albicans* and photographs of effects of AMB-loaded NPs on the activity of *C. albicans* as confirmed by annexin V/PI staining (fluorescence microscopy; 24 hours, 48 hours, and 72 hours; ×400). (**B**) Representative flow cytometry of apoptosis and necrosis after annexin V and PI staining of *C. albicans* treated with AMB-loaded NPs for 24 hours, 48 hours, and 72 hours.
Abbreviations: AMB, amphotericin B; FITC, fluorescein isothiocyanate; NP, nanoparticle; PI, propidium iodide.

(Table 3). There were no fungi in the kidney and liver of the AMB-NPs group, and the amount of fungi in the lung and heart was also significantly reduced when compared with the control group.

Histologic analysis

The heart, kidney, lung, and liver were harvested and processed for histologic examination. Representative photographs of AMB-NP-treated mice are shown in Figure 5 and Figure 6. As shown in Figure 5, the liver and kidney of the AMB-NP-treated mice were uninfected by fungus, but there were fungi in the heart, and the infected myocytes underwent degeneration or even necrosis.

In the animal studies, the lung structure in the normal changes to the control group were well defined, without discernible damage or edema, and the trachea and blood vessels were not infiltrated by inflammatory cells (Figure 6A). However, the lung tissues and bronchial structures in *C. albicans*-infected mice were disturbed due to hemorrhage and edema, with bronchial and vascular walls that were thickened and infiltrated by a considerable number of inflammatory cells (Figure 6B), and in the PBS group and PLGA-TPGS NP group, the irregular structures and inflammatory cells infiltration were obvious, the bronchial and vascular walls were thickened, and numerous fungi infiltrated the lung tissues. These histological features were the same as those in

Table 3 Survived rate and CFU in different organs of *Candida albicans*-infected mice

	Log CFU/gram tissue (n=3)				Survival rate[c] (%) (n=20)
	Lung	Heart	Kidney	Liver	
Control	3.63±0.55	2.21±0.32	3.88±0.53	2.31±0.57	0.0
PBS	3.65±0.42	2.17±0.33	3.90±0.56	2.29±0.52	0.0
Free AMB	2.12±0.04[a]	1.02±0.12[a]	1.04±0.22[a]	1.23±0.23[a]	30.0
PLGA-TPGS	3.59±0.51	2.02±0.15	3.67±0.48	2.30±0.93	0.0
AMB-PLGA-TPGS	1.13±0.03[a]	0.98±0.05[a]	Nil[b]	Nil[b]	80.0

Notes: Data are expressed as mean ± SEM from three independent experiments. One-way analysis of variance was used for comparisons among groups, and two-tailed *t*-test was used for comparisons between two groups. [a]$P<0.05$; [b]$P<0.001$. [c]Survival rate at 20 days after therapy (n=20).
Abbreviations: AMB, amphotericin B; CFU, colony-forming units; PBS, phosphate buffer solution; PLGA, poly(d, l-lactide-co-glycolide); SEM, standard error of the mean; TPGS, d-α-tocopheryl polyethylene glycol 1000 succinate.

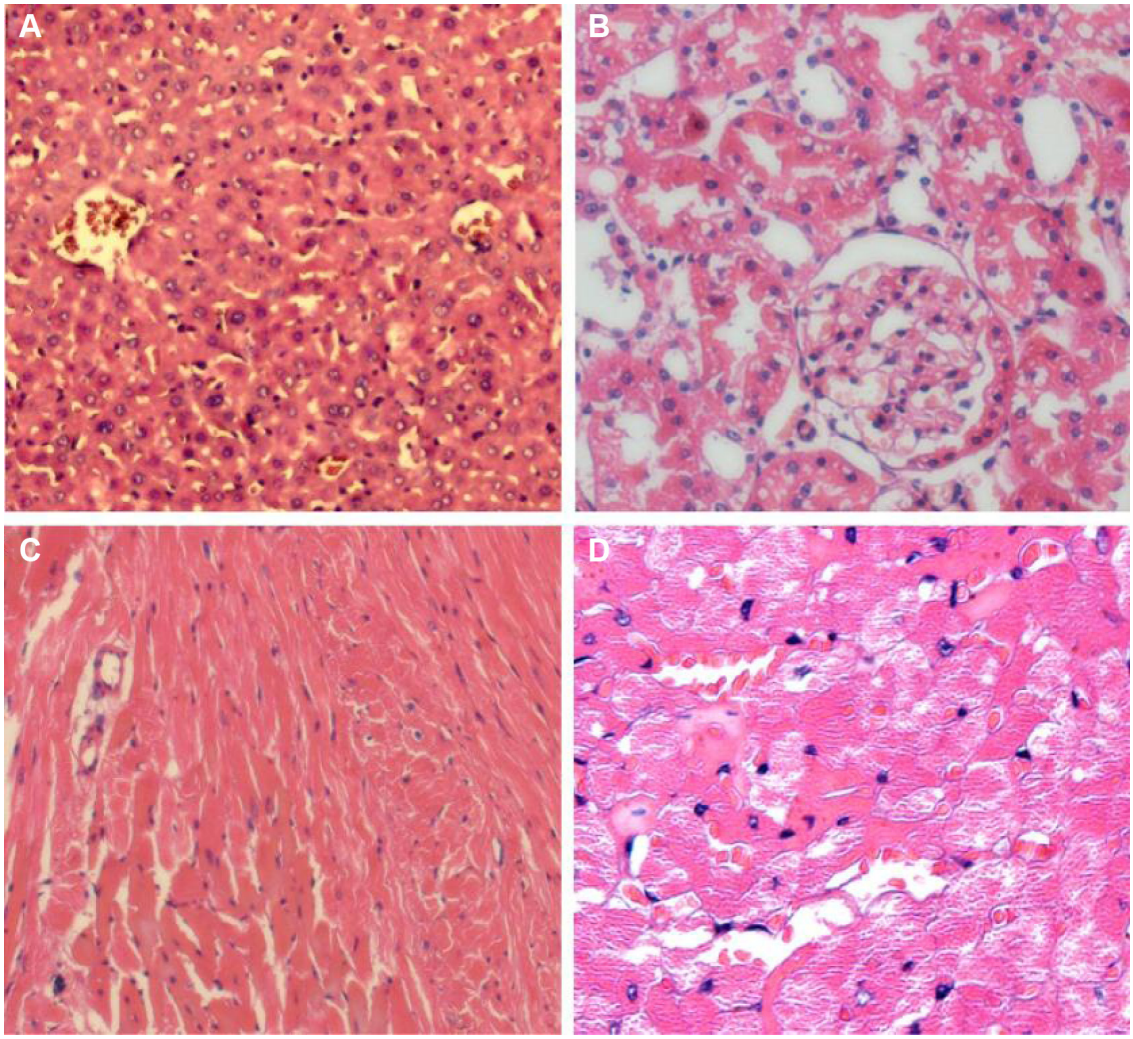

Figure 5 Representative HE staining of *Candida albicans*-infected mice after AMB-NP-treatment.
Notes: The liver (**A**) and kidney (**B**) of the AMB-NP-treated mice had no fungus. (**C**) *C. albicans*-uninfected heart section of the mice. (**D**) *C. albicans*-infected heart section of the AMB-NP-treated mice and the infected myocytes underwent degeneration, or even necrosis (×400).
Abbreviations: AMB, amphotericin B; HE, hematoxylin and eosin; NP, nanoparticle.

C. albicans-infected mice treated with PBS and null-loaded NPs (Figure 6C and D). However, in the free AMB group and AMB-NPs group, the histologic findings were significantly improved when compared with non-treated *C. albicans*-infected mice, although there was mild histologic change in the lung tissues in both groups (such as infiltration of several inflammatory cells in the lung), and the pulmonary interstitial edema was also dramatically improved (Figure 6E and F). Moreover, the lung lesions of the AMB-NP group were significantly improved and the fungal burden reduced markedly when compared with free AMB group (Figure 4F).

Discussion

Pulmonary fungal infections are serious life-threatening diseases. To improve the treatment of pulmonary infections, several antifungal agents, including echinocandin, pyrimidine, and polyene have been developed. AMB is a systemic antifungal polyene, having broad spectrum and favorable antifungal activity against a variety of fungi and fungal infections, such as *Cryptococcus neoformans, C. albicans, Histoplasma capsulatum fungus, Coccidioides immitis, blastomycosis dermatitis, Mucor,* and *Aspergillus.*[19,22,23] Thus, AMB has become the most important antifungal agent in clinical therapy of fungal infection.[22,23] However, the safety of AMB remains an important concern. AMB has common ADRs of the digestive system and serious toxicity to the kidney and may even cause leukopenia and liver damage.[22,24] Moreover, its wide application is limited due to poor solubility in aqueous solution. Thus, the development of alternative drugs is a priority in the therapy of fungal infection.

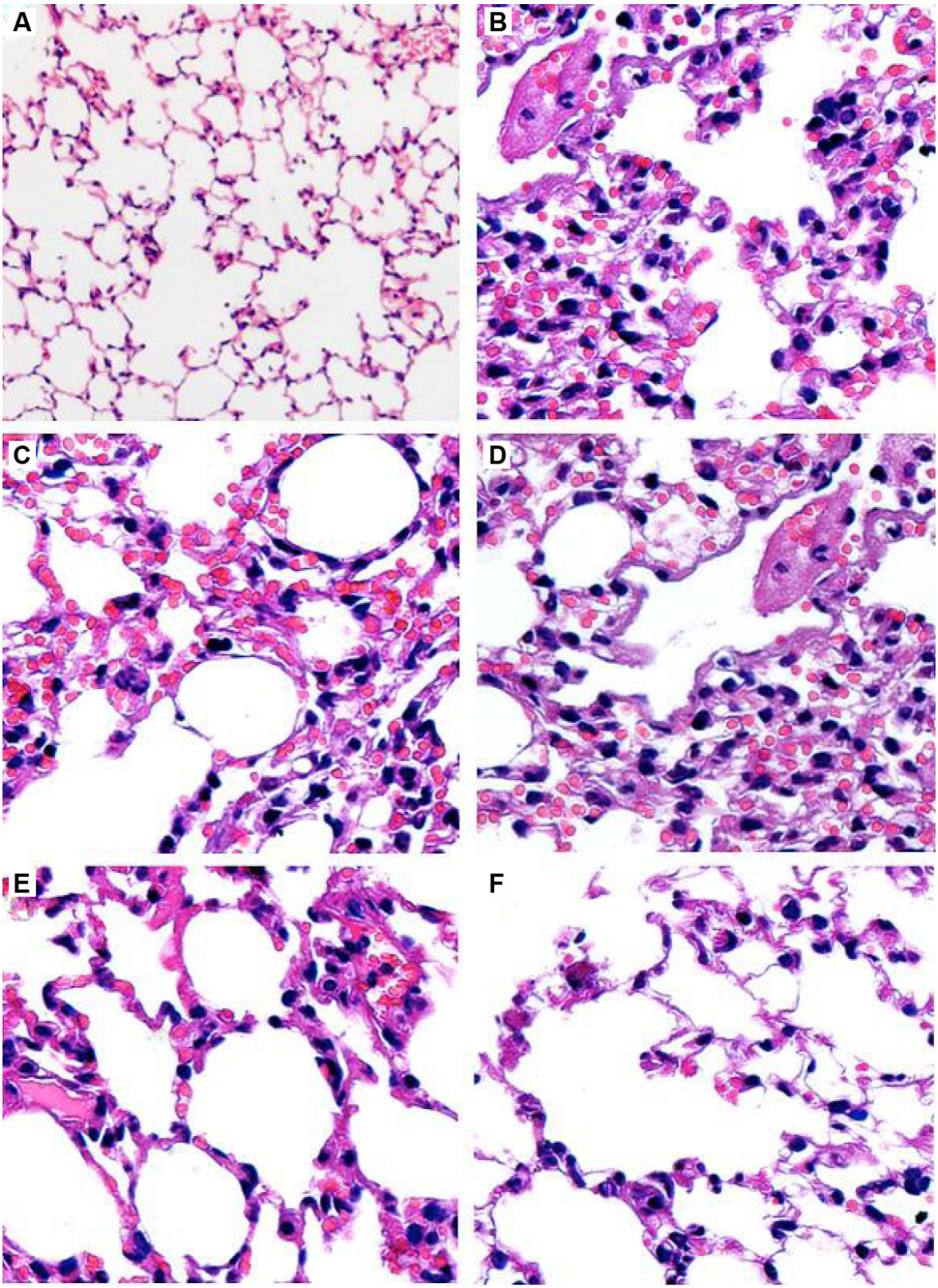

Figure 6 Lung sections of *Candida albicans*-infected mice.
Notes: (**A**) Normal lung section with HE staining (×100). (**B**) Lung section of *C. albicans*-infected mice after PAS staining and hematoxylin staining showed pulmonary interstitial edema with numerous intracellular and extracellular, round to oval, elongated, thin-walled, yeast-like, and moniliform hyphal organisms (×400). (**C** and **D**) Lung section of *C. albicans*-infected mice treated with PBS or null-loaded NPs after PAS staining and hematoxylin staining showed similar findings to those in untreated mice (×400). (**E** and **F**) Lung sections of *C. albicans*-infected mice treated with free AMB (1 mg/kg/day for 10 days, totalizing 10 mg/kg/animal) or AMB-NPs (10.0 mg/kg on the first, seventh, and 14th days, and totaling 30 mg/kg/animal, equivalent to 3.0 mg/kg/animal free AMB) after PAS staining and hematoxylin staining showed significant improvements of pulmonary interstitial edema and reduced amount of fungi (×400).
Abbreviations: AMB, amphotericin B; HE, hematoxylin and eosin; NP, nanoparticle; PAS, periodic acid-Schiff; PBS, phosphate buffer solution.

In recent years, a lot of attention has been paid to the biodegradable polymeric NPs as drug carriers because they have many advantages, including a stable structure, high solubility, desirable biodistribution, as well as reasonable pharmacokinetics.[25] Especially, the use of PLGA-based NPs as a delivery vehicle for high hydrophobicity drugs has been extensively reported. The present study aimed to investigate whether AMB loaded onto novel PLGA-TPGS NPs had higher drug solubility and/or fewer ADRs than free AMB, without affecting the therapeutic efficacy of AMB.

The physical properties of AMB-NPs were examined by FESEM. Results showed all the prepared particles were homogeneously spherical and smooth (Figure 1). Table 1 summarizes the size, polydispersity, ZP, and EE% for the different NPs. The size of the AMB-NPs was 122.7±3.9 nm, which is very conducive to cellar absorption and internalization.[26] The EE% of the AMB-NPs was 84.37% (Table 1). The surface charge of NPs is an important physicochemical parameter that can influence their stability in a solution and the interaction between NPs and cell membrane in vivo. In the case of a combined electrostatic and steric stabilization, a minimum ZP of ±20 mV is desirable.[26,27] As shown in Table 1, the ZP of AMB-NPs was just in the range of ±20 mV. AMB release from the PLGA-TPGS NPs in PBS was biphasic, with an initial increase of 45% in the first 12 days, followed by a flat phase in the following 18 days (Figure 2). The initial increase was attributed to the release of the drug from the particle surface. Thereafter, the drug was released due to diffusion and particle degradation.[26,27] The therapeutic efficacy may increase with the increase in the AMB release. The bulky structure and large surface area of AMB-NPs make them an excellent solubilizer, emulsifier, and bioavailable enhancer of hydrophobic drugs.[19,28] The NPs have high affinity to cells and can be rapidly internalized by these cells, and then AMB is gradually released from NPs in a sustained manner.[29] Our results suggested that PLGA-TPGS NPs were an excellent polymer carrier of hydrophobic drugs.

To investigate whether the drug effectively induces apoptosis and necrosis of *C. albicans*, the apoptosis and necrosis of AMB-NP-treated *C. albicans* cells were detected after annexin V-FITC and PI double-staining. Following AMB-NPs (5.0 μg/mL, equivalent to 0.5 μg/mL AMB) exposure at 37°C for 24 hours, about 65% of *C. albicans* were positive for annexin V-FITC, while only about 35% for PI. With the prolongation of incubation with AMB-NPs, the rates of *C. albicans* positive for annexin V and PI increased progressively. These results suggest that AMB-NPs may exert antifungal effect via inducing the apoptosis and necrosis of *C. albicans*. Moreover, the antifungal effects of AMB-NPs are better than those of free AMB in vitro.

In addition, we also investigated the antifungal effects of free AMB and AMB-NPs in vivo. As shown in Table 3, the CFU/g in lung tissue was detected in mice treated with free AMB, AMB-NPs, PLGA-TPGS NPs, and PBS. The mice of the free AMB and AMB-NPs groups had a markedly decreased lung CFU when compared with the PBS group and PLGA-TPGS NP group. Moreover, the AMB-NPs group showed significantly reduced fungal burden in the lungs when compared with the free AMB group, and the survival ratio in the AMB-NPs group was also remarkably higher than that in other groups (Table 3). Furthermore, the improvement in the histopathological findings was also consistent with the antifungal effects of free AMB and AMB-NPs. HE staining showed the *C. albicans*-infected lung had inflammatory cell infiltration (Figure 5), swelling of lung tissues, pulmonary interstitial edema, and obvious fungi. PLGA-TPGS NPs neither alleviated these pathological changes in the lungs nor reduced the amount of fungi (Figure 5 and Table 3). However, these lesions were improved in mice treated with free AMB, and in the mice treated with PLGA-TPGS NPs, these lesions were almost undetectable. These results suggest that the antifungal effects of AMB-NPs were better than those of free AMB. This also suggests that the frequency of antifungal therapy is lower for AMB-NPs than that for free AMB, when the therapeutic efficacy is comparable.

In all, AMB-NPs have at least the same or even better antifungal effects than free AMB does, as demonstrated by the improved histological changes of important organs, reduction in mortality, decreased amount of fungi in the lung, and increased apoptosis and necrosis of *C. albicans*. Further studies are required to investigate the specific mechanism and cost-effectiveness of antifungal therapy with AMB-NPs.

Acknowledgments

This study was supported by the Open Research Fund Program of the State Key Laboratory of Virology of the People's Republic of China (grant number 2014KF004), Guangdong Provincial Health Department Fund (grant number A2011224), the National High Technology Research and Development Program (863 Program) (grant number 2011AA02A111), and the 2011 Infectious Disease Prevention and Control Technology major project (grant number 2012ZX10004903).

Disclosure

The authors report no conflicts of interest in this work.

References

1. Pili FM, Erriu M, Piras A, Garau V. Application of the novel method in the diagnosis and treatment of median rhomboid glossitis Candida-associated. *Eur J Dent*. 2014;8(1):129–131.
2. Tariq TM. Bacteriologic profile and antibiogram of blood culture isolates from a children's hospital in Kabul. *J Coll Physicians Surg Pak*. 2014;24(6):396–399.
3. de Lima CT, Magalhães V. Abscess resulting from Mycobacterium kansasii in the left thigh of AIDS patient. *An Bras Dermatol*. 2014;89(3):478–480.
4. Tapia CV, Falconer M, Tempio F, et al. Melanocytes and melanin represent a first line of innate immunity against Candida albicans. *Med Mycol*. 2014;52(5):445–454.
5. Bonifaz A, Tirado-Sánchez A, Graniel MJ, Mena C, Valencia A, Ponce-Olivera RM. The efficacy and safety of sertaconazole cream (2 %) in diaper dermatitis candidiasis. *Mycopathologia*. 2013;175(3–4):249–254.
6. Quinteros AR, Fica CA, Abusada AN, Muñoz CL, Novoa MC, Gallardo AC. [Amphotericin B deoxycholate prescription and adverse events in a Chilean university hospital]. *Rev Chilena Infectol*. 2010;27(1):25–33. Spanish.
7. Van de Ven H, Paulussen C, Feijens PB, et al. PLGA nanoparticles and nanosuspensions with amphotericin B: Potent in vitro and in vivo alternatives to Fungizone and AmBisome. *J Control Release*. 2012;161(3):795–803.
8. Jain JP, Kumar N. Development of amphotericin B loaded polymersomes based on (PEG)(3)-PLA co-polymers: Factors affecting size and in vitro evaluation. *Eur J Pharm Sci*. 2010;40(5):456–465.
9. Nahar M, Jain NK. Preparation, characterization and evaluation of targeting potential of amphotericin B-loaded engineered PLGA nanoparticles. *Pharm Res*. 2009;26(12):2588–2598.
10. Choi KC, Bang JY, Kim PI, Kim C, Song CE. Amphotericin B-incorporated polymeric micelles composed of poly(d,l-lactide-co-glycolide)/dextran graft copolymer. *Int J Pharm*. 2008;355(1–2):224–230.
11. Kassab R, Parrot-Lopez H, Fessi H, Menaucourt J, Bonaly R, Coulon J. Molecular recognition by Kluyveromyces of amphotericin B-loaded, galactose-tagged, poly (lactic acid) microspheres. *Bioorg Med Chem*. 2002;10(6):1767–1775.
12. Jain JP, Jatana M, Chakrabarti A, Kumar N. Amphotericin-B-loaded polymersomes formulation (PAMBO) based on $(PEG)_3$-PLA copolymers: an in vivo evaluation in a murine model. *Mol Pharm*. 2011;8(1):204–212.
13. Khan MJ, Rizwan Alam M, Waldeck-Weiermair M, et al. Inhibition of autophagy rescues palmitic acid-induced necroptosis of endothelial cells. *J Biol Chem*. 2012;287(25):21110–21120.
14. Shirazi F, Kontoyiannis DP. The calcineurin pathway inhibitor tacrolimus enhances the in vitro activity of azoles against Mucorales via apoptosis. *Eukaryot Cell*. 2013;12(9):1225–1234.
15. Shirazi F, Pontikos MA, Walsh TJ, Albert N, Lewis RE, Kontoyiannis DP. Hyperthermia sensitizes Rhizopus oryzae to posaconazole and itraconazole action through apoptosis. *Antimicrob Agents Chemother*. 2013;57(9):4360–4368.
16. Da Silva CR, Magalhães HIF, de Moraes MO, Nobre HV Junior. Susceptibility to amphotericin B of Candida spp. strains isolated in Ceará, Northeastern Brazil. *Rev Soc Bras Med Trop*. 2013;46(2):244–245.
17. Gharib A, Faezizadeh Z, Mohammad Asghari H. Preparation and antifungal activity of spray-dried amphotericin B-loaded nanospheres. *Daru*. 2011;19(5):351–355.
18. Burgess BL, He Y, Baker MM, et al. NanoDisk containing super aggregated amphotericin B: a high therapeutic index antifungal formulation with enhanced potency. *Int J Nanomedicine*. 2013;8:4733–4743.
19. Bhavikatti SK, Bhardwaj S, Prabhuji ML. Current applications of nanotechnology in dentistry: a review. *Gen Dent*. 2014;62(4):72–77.
20. Lakkakula JR, Maçedo Krause RW. A vision for cyclodextrin nanoparticles in drug delivery systems and pharmaceutical applications. *Nanomedicine (Lond)*. 2014;9(6):877–894.
21. Das J, Das S, Paul A, Samadder A, Khuda-Bukhsh AR. Strong anticancer potential of nano-triterpenoid from Phytolacca decandra against A549 adenocarcinoma via a Ca(2+)-dependent mitochondrial apoptotic pathway. *J Acupunct Meridian Stud*. 2014;7(3):140–150.
22. Fernandez-Flores A, Saeb-Lima M, Arenas-Guzman R. Morphological findings of deep cutaneous fungal infections. *Am J Dermatopathol*. 2014;36(7):531–553; quiz 554.
23. Paramythiotou E, Frantzeskaki F, Flevari A, Armaganidis A, Dimopoulos G. Invasive fungal infections in the ICU: how to approach, how to treat. *Molecules*. 2014;19(1):1085–1119.
24. Horwitz E, Shavit O, Shouval R, Hoffman A, Shapiro M, Moses AE. Evaluating real-life clinical and economical burden of amphotericin-B deoxycholate adverse reactions. *Int J Clin Pharm*. 2012;34(4):611–617.
25. Nahar M, Dubey V, Mishra D, Mishra PK, Dube A, Jain NK. In vitro evaluation of surface functionalized gelatin nanoparticles for macrophage targeting in the therapy of visceral leishmaniasis. *J Drug Target*. 2010;18(2):93–105.
26. Tan SW, Billa N. Lipid effects on expulsion rate of amphotericin B from solid lipid nanoparticles. *AAPS Pharm Sci Tech*. 2014;15(2):287–295.
27. Tang X, Cai S, Zhang R, et al. Paclitaxel-loaded nanoparticles of star-shaped cholic acid-core PLA-TPGS copolymer for breast cancer treatment. *Nanoscale Res Lett*. 2013;8(1):420.
28. Hou Z, Wei H, Wang Q, et al. New method to prepare mitomycin C loaded PLA-nanoparticles with high drug entrapment efficiency. *Nanoscale Res Lett*. 2009;4(7):732–737.
29. Clemons KV, Ranney DF, Stevens DA. A novel heparin-coated hydrophilic preparation of amphotericin B hydrosomes. *Curr Opin Investig Drugs*. 2001;2(4):480–487.